Journal of New Technology and Materials (JNTM)
J. New Technol. Mater.
Vol. 09, N°01 (2019)89-96

OEB Univ. Publish. Co.

Heat transfer study in binary alloys solidification Pb-Sn and Pb-Sb

S. Adouane, A. Kerboub* and E. Belbacha

Physico-Chimical studies of materials Laboratory, faculty of matter science, University Batna1, Algeria

*Corresponding author, email: kerboubhako@gmail.com

Received date: March 05, 2019 ; revised date: May 26, 2019 ; accepted date: May 31, 2019

Abstract

Simulation of solidification processes has been of interest for a number of years not only because of its scientific value in understanding pattern formation in nature but also because of its importance in many technological applications. The classical Stefan problem is well accepted for modeling the solidification of pure materials and alloys. The two-dimensional model is based on the resolution of heat transfer equation, including the latent heat term. For solving this equation a finite volume method was used. The obtained model from solving the heat transfer equation has leadresults for the temperature changes over cooling time for Antimony-Lead and Lead-Tin alloys at various compositions. The obtained cooling curves were compared with the literature results, and they show a good agreement.

Keywords: Solidification; Heat transfer; Nucleation; Growth morphologies; Liquid/solid interface.

1. Introduction

The formation of solids is still incompletely understood, although it has been the subject of much research, which focused on metals and alloys. These are the product of a process that is known as solidification. The modeling of solidification is mainly concentrated on the calculation of the evolution of the thermal field in castings.

The solidification process is induced by the progress of an interface between the liquid and the solid phase[1,2] Interfacial stability was first studied by Mullins and Sekerka in 1963 for diluted systems. After, other authors have extended this study. The liquid-solid interface can take different growth morphologies (flat, cell or dendritic) all depends on the solidification conditions [3-5].

The materials solidification, which involves essentially a rearrangement of atoms or molecules in the liquid state or solid state and which controls, in a large extent, the formation of microstructures [6] , is an exothermic transformation and the latent heat must be extracted from the system so that the liquid-solid transformation can proceed in the liquid phase [7] .

This phase transformation involves two steps further, germination and growth [8-9].The first is the formation, within the liquid, of small clusters called nuclei, in particular sites, from which solidification can start. These germs can be stable or metastable depending on whether they attain the stability condition or not, homogeneous or heterogeneous depending on whether the metal was pure or it contain impurities (mold surface, foreign particles, ...) [10-13]. Conditions leading to germination are therefore of utmost importance in determining the characteristics of the molded microstructure [14].

Once the germs built, they will continue their growth, in the second step, which is characterized by the development of these germs in observable morphological features, at the expense of the liquid, by building what is called grain while preserving their orientation [15].

As the solidification can be described in terms of mass and heat transfer, we are interested, in this work, to the heat transfer by trying to model the solidification at any point of the room studied, using the Gulliver–Scheil solid-fraction equation [16]. We will use these alloys:

- Lead-Tin whose melting point is low and that it has better corrosion resistance [17].
- Lead-Antimony where the addition of antimony in lead creates alloys which have a very high resistance. These alloys retain a shinyappearance in the air for a larger time compared to smooth lead alloys [18].

In this paper, we have resolved the heat transfer equation including latent heat term, which allows obtaining results concerning the temperature changes over cooling time for Antimony-Lead and Lead-Tin alloys at each point in casting. We have used the finite volume method to solve the heat transfer equation, including the latent heat term, for both alloys Antimony-Lead and Lead-Tin, which make this work novel, unlike other previous works in this field of research.

2. Computational Methodology

The heat transfer flow has importance in different engineering applications such as the solidification process and is described by the equation of heat diffusion[19], which, much research has focused on solving this equation, with or without a source term.

Analytical solutions of this equation without source term have been proposed for some geometry [20]. Others have solved this equation with a source term like Li [21-25]

In this case, the problem studied is to solve the heat diffusion equation, with a source term related to the release of latent heat, to obtain a good representation of the thermal field in a casting by assuming a single path of solidification using a mesh of 50 x 50 mm.

$$div\,(K\ \overrightarrow{grad}\ T) + \dot{Q} = \rho.c_p.\frac{\partial T}{\partial t} \quad (1)$$

$$\dot{Q} = \rho L.\frac{\partial f_s}{\partial t} \quad (2)$$

$$f_s = \frac{1}{1-k}\left(\frac{T - T_{liq}}{T - T_f}\right) \quad (3)$$

Where:

T is the temperature, $\dot{Q}$ the source term, L the latent heat, f_s the solid fraction, T_f the melting temperature, T_{liq} the liquidus temperature, K, c_p and ρ are respectively the thermal conductivity, specific heat and density. These can be described by the following formula as:

$$c_p = (1 - f_s)c_{pl} + f_s c_{ps}. \quad (4)$$

$$\rho = (1 - f_s)\rho_l + f_s \rho_s. \quad (5)$$

$$K = (1 - f_s)K_l + f_s K_s. \quad (6)$$

The indices l and s refer to liquid and solid phases.

The modeling is based on solving a set of equations in 2D using the finite volume method for the discretization [26-28, 30-32], and using the method of Jacobi to solve the linear system obtained after discretization:

$$T_{i,j}^{(k+1)} = \frac{1}{a_p}\left(a_e.T_{i+1,j}^{(k)} + a_w.T_{i-1,j}^{(k)} + a_n.T_{i,j+1}^{(k)} + a_s.T_{i,j-1}^{(k)} + a_{p_0}.T_{i,j}^{(k)}\right) \quad (7)$$

With a_e, a_w, a_n, a_s are the coefficients referring to nodes of the mesh, a_{p_0} is function of c_p pand ρ, a_p is function of these coefficients.

After including the following boundary conditions, wrote a program in Fortran 6.6 whose steps are summarized in the flowchart of Figure.

$$K\left(\frac{\partial T}{\partial x}\right)_{x=0} = q. \quad (8)$$

$$K\left(\frac{\partial T}{\partial x}\right)_{x=x\max} = q. \quad (9)$$

$$-K\left(\frac{\partial T}{\partial y}\right)_{y=0} = h.(T - T_{ext}). \quad (10)$$

$$K\left(\frac{\partial T}{\partial y}\right)_{y=y\max} = 0. \quad (11)$$

Fig.1. Flowchart showing the computer code.

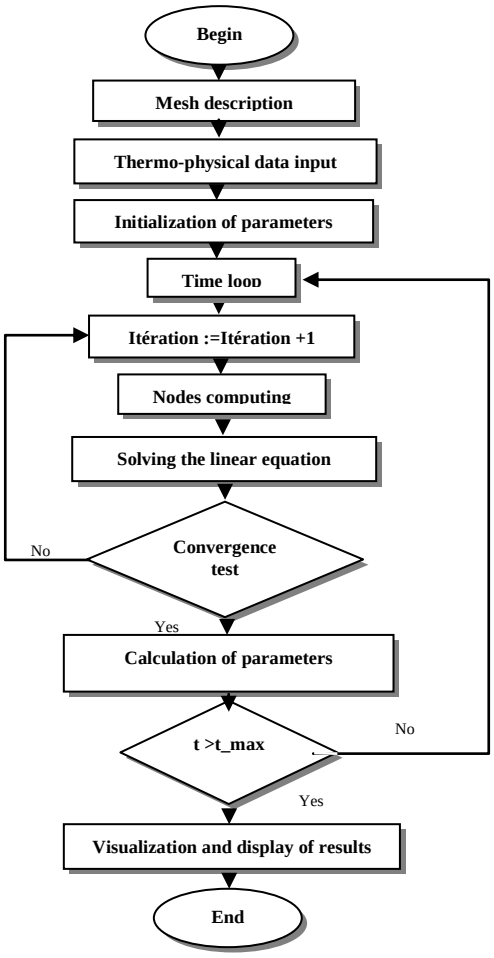

3. Results and discussion

Calculations were made for lead-tin alloy with Sn-5wt%Pb, Sn-15wt%Pb, Sn-20wt%Pb and Sn-25wt%Pb. The thermo-physical properties of these alloys are reported in Table 1.

	Sn-5wt.%Pb	Sn-15wt.%Pb	Sn-20wt.%Pb	Sn-25wt.%Pb
$K_s (W(m°K)^{-1})$	65	62.2	60.5	58.9
$K_l (W(m°K)^{-1})$	32.8	32.5	32.3	32.3
$c_{ps} (J(kg°K)^{-1})$	216	207.3	202.8	198.2
$c_{pl} (J(kg°K)^{-1})$	253	240.9	234.8	228.8
$\rho_s (kg\ m^{-3})$	7502	7906	8108	8310
$\rho_l (kg\ m^{-3})$	7183	7551.7	7735.6	7919.5
$L\ (J\ kg^{-1})$	58985	55534	53809	52083.8
$T_L (°C)$	220	210	206	200
$T_E (°C)$	183	183	183	183
$T_f (°C)$	232	232	232	232
k	0.0656	0.0656	0.0656	0.0656

The cooling curves obtained for the four compositions used in the solidification of these alloys are shown in Figure 2. These curves are plotted at (30 x 30) mm and compared with experimental curves [29].

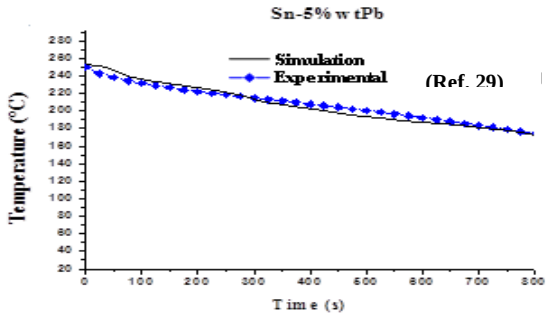

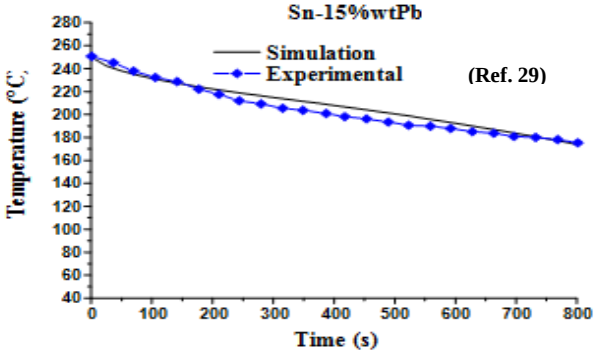

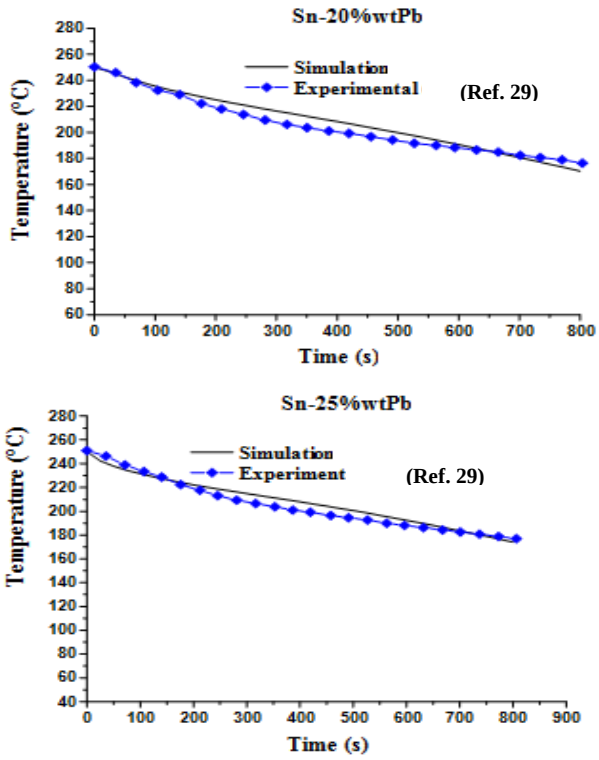

Figure2. Variation of the temperature as a function of cooling time for the Sn-Pb alloy.

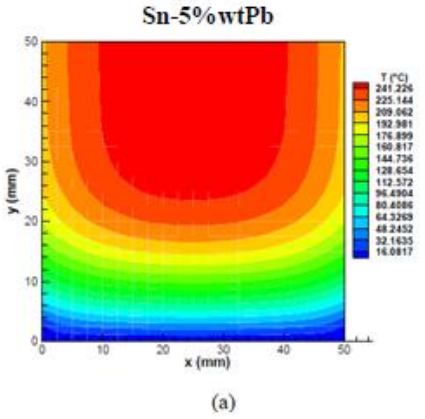

(a)

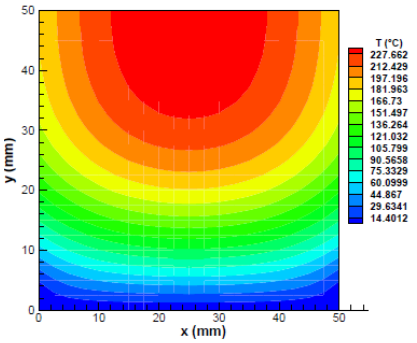

(b)

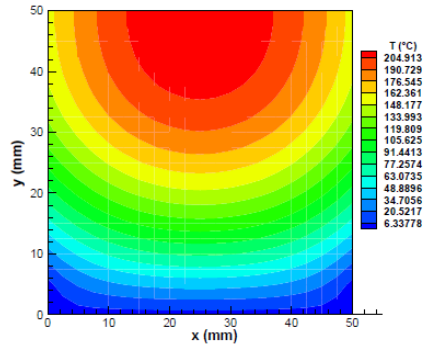
T (°C)
204.913
190.729
176.545
162.361
148.177
133.993
119.809
105.625
91.4413
77.2574
63.0735
48.8896
34.7056
20.5217
6.33778
y (mm)
x (mm)

(c)

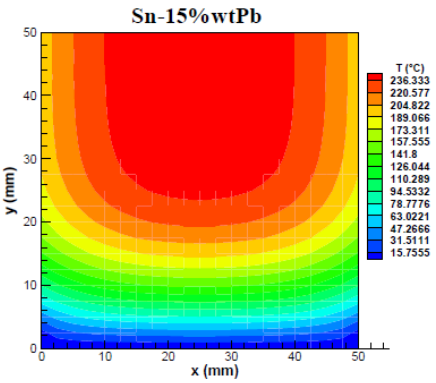
Sn-15%wtPb
T (°C)
236.333
220.577
204.822
189.066
173.311
157.555
141.8
126.044
110.289
94.5332
78.7776
63.0221
47.2666
31.5111
15.7555
y (mm)
x (mm)

(a)

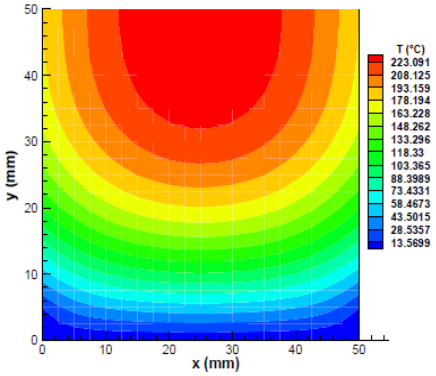
T (°C)
223.091
208.125
193.159
178.194
163.228
148.262
133.296
118.33
103.365
88.3989
73.4331
58.4673
43.5015
28.5357
13.5699
y (mm)
x (mm)

(b)

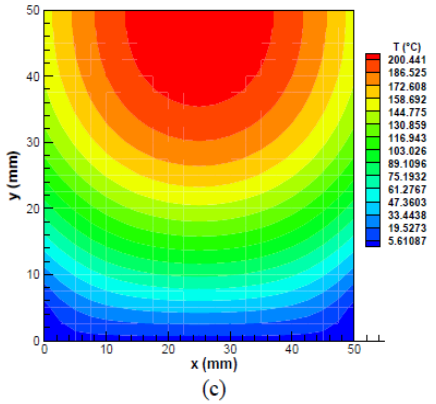
T (°C)
200.441
186.525
172.608
158.692
144.775
130.859
116.943
103.026
89.1096
75.1932
61.2767
47.3603
33.4438
19.5273
5.61087
y (mm)
x (mm)

(c)

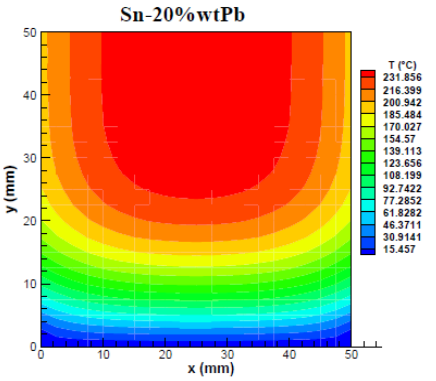
Sn-20%wtPb
T (°C)
231.856
216.399
200.942
185.484
170.027
154.57
139.113
123.656
108.199
92.7422
77.2852
61.8282
46.3711
30.9141
15.457
y (mm)
x (mm)

(a)

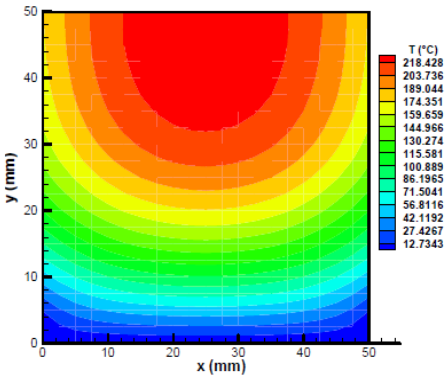
T (°C)
218.428
203.736
189.044
174.351
159.659
144.966
130.274
115.581
100.889
86.1965
71.5041
56.8116
42.1192
27.4267
12.7343
y (mm)
x (mm)

(b)

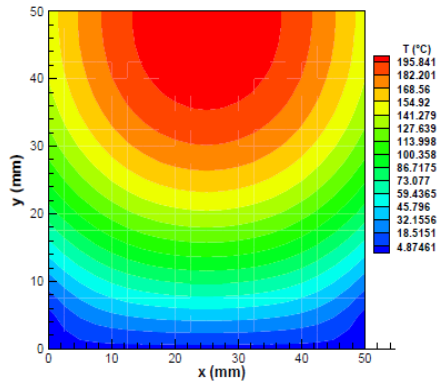
T (°C)
195.841
182.201
168.56
154.92
141.279
127.639
113.998
100.358
86.7175
73.077
59.4365
45.796
32.1556
18.5151
4.87461
y (mm)
x (mm)

(c)

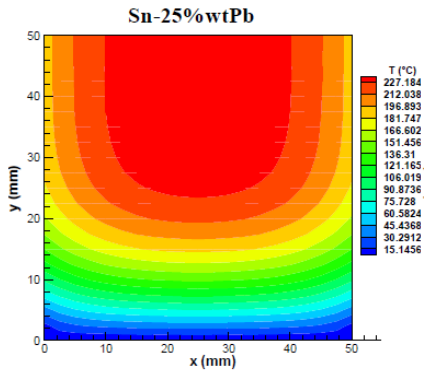
Sn-25%wtPb
T (°C)
227.184
212.038
196.893
181.747
166.602
151.456
136.31
121.165
106.019
90.8736
75.728
60.5824
45.4368
30.2912
15.1456
y (mm)
x (mm)

(a)

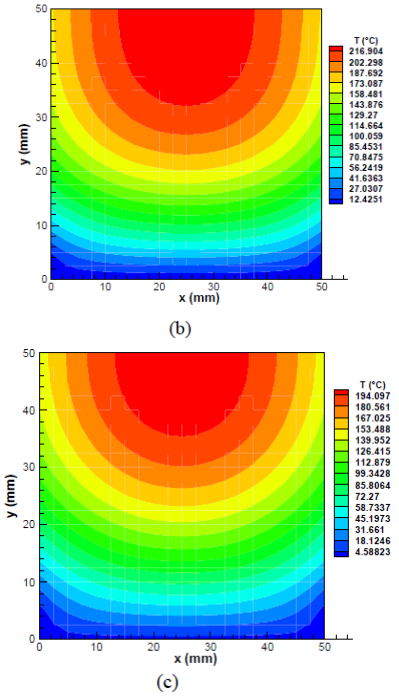

Figure 3. Temperature fields at selected instants during the solidification for the four used compositions: (a) T=50 s, (b)=100 s, (c)=150s.

Regarding the lead-antimony alloy, calculations were performed for three compositions Pb-0,3wt%Sb, Pb0.85 wt % Sb and Pb-1.9 wt % Sb where the thermo-physical data are presented in Table 2.

The authors obtained the curves shown in Figure 4. These curves are in good agreement with the experimental curves [3].

	Pb-0,3wt.%Sb	Pb-0.85wt.%Sb	Pb-1.9wt.%Sb
$K_s (W(m°K)^{-1})$	33.0	32.9	32.8
$K_l (W(m°K)^{-1})$	29.7	29.6	29.5
$c_{ps} (J(kg°K)^{-1})$	130	130.5	131.3
$c_{pl} (J(kg°K)^{-1})$	138.5	139	140.1
$\rho_s (kgm^{-3})$	11326	11300	11251.5
$\rho_l (kgm^{-3})$	10665	10642	10598.3
$L\ (Jkg^{-1})$	26615	27368	28804.1
$T_L (°C)$	326.6	325.2	322
$T_E (°C)$	251.7	251.7	251.7
$T_f (°C)$	327.4	327.4	327.4
k	0.3125	0.3125	0.3125

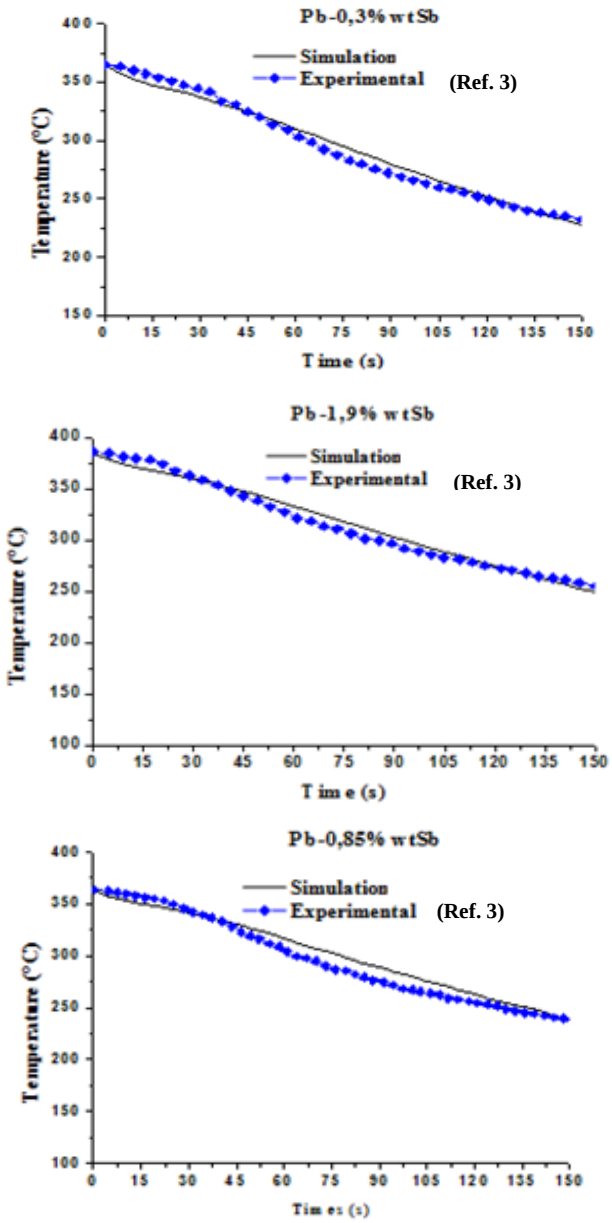

Figure 4. Variation of the temperature as a function of cooling time for the Pb-Sb alloy.

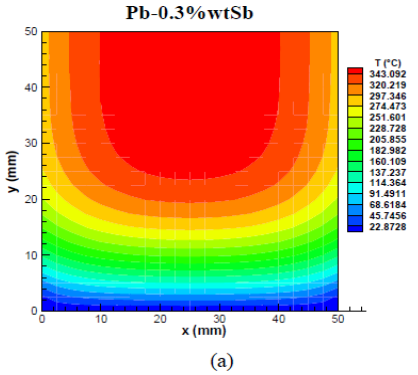

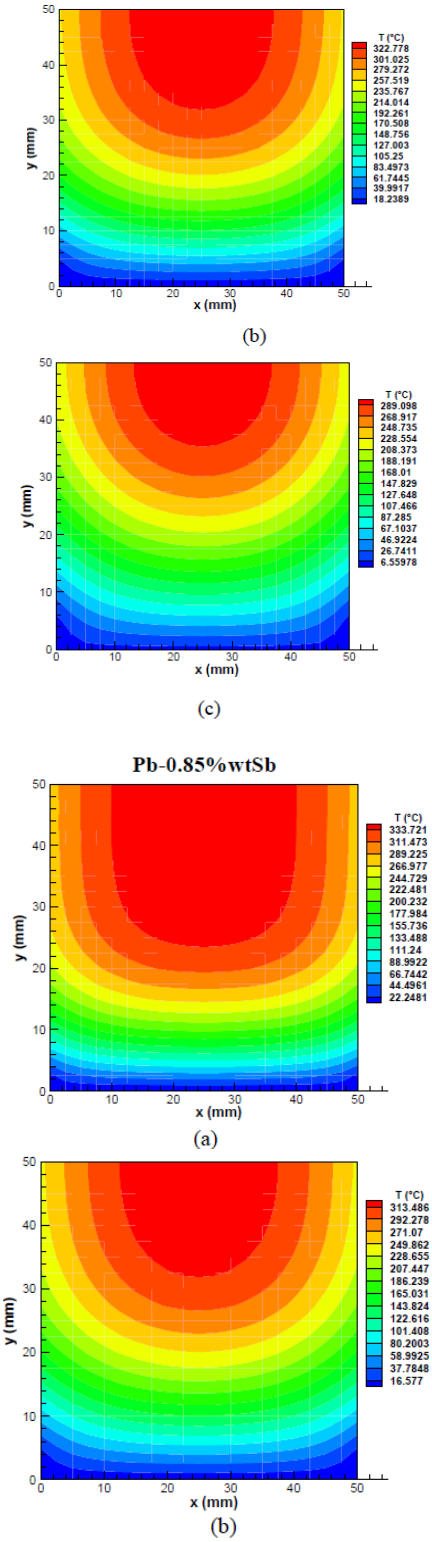

Figure 5. Temperature fields at selected instants during the solidification for the three used compositions:
(a) T=50 s, (b)=100 s, (c)=150s.

4. Conclusion

The solidification modeling, including the study of heat transfer in solidified metal, allows us to obtain certain information concerning the evolution of thermal field in a cast during its growth over a time.

In contrast to classical solidification model used to calculate the temperature variation during the cooling time, the presented two-dimensional model includes the latent heat term in the heat transfer equation like other works in this field of research, but the equation is solved by using finite volume method which is based on approximations of integrals.

The model obtained from this study is applied to different alloys at various compositions: Tin-Lead (Sn-5 wt % Pb, Sn-15 wt % Pb, Sn-20 wt % Pb, Sn-25 wt % Pb,) and Antimony-Lead (Pb-0,3 wt % Sb, Pb-0,85 wt % Sb and Pb-1,9 wt % Sb).

The obtained curves for the variation of temperature versus time cooling are in good agreement with the experimental curves presented by the authors cited above.

Nomenclature

$K_s\,(W(m°K)^{-1})$: thermal conductivity-solid phase

$K_l\,(W(m°K)^{-1})$:thermal conductivity-liquid phase

$c_{ps}\,(J(kg°K)^{-1})$:specific heat-solid phase

$c_{pl}\,(J(kg°K)^{-1})$:specific heat-liquid phase

$\rho_s\,(kgm^{-3})$: density-solid phase

$\rho_l\,(kgm^{-3})$:density-liquid phase

$L(Jkg^{-1})$: latent heat in melting

$T_L\,(°C)$: liquidus temperature

$T_E\,(°C)$:eutectic temperature

$T_f\,(°C)$: melting temperature

k: Partition coefficient.

References

[1] B. Caroli, C. Caroli, C. Misbah, B. Roulet, J. Phy.46, 4(1985)01-413.

[2]M. E. Glicksman, Principles of solidification: An introduction to modern casting and crystal growth concepts (Springer Science+Business Media LLC, New York, 2011).

[3] D. M. Rosa, J. E. Spinelli, I. L. Ferreira, A. Garcia, J. Alloys& Compounds.422, (2006)227–238.

[4] H. Nguyen Thi, Y. Dabo, B. Drevet, M.D. Dupouy, D. Camel, B. Billia, J.D. Hunt, A. Chilton, J. Crystal. Growth.281, (2005)654–668.

[5] W. Kurz, B. Giovanola, R. Trivedi, Acta. Metall.34, (1986) 823-830.

[6] A. Ludwig, W. Kurz, Acta Mater44, (1996) 3643-3654.

[7] T. R. Vijayaram, S. Sulaiman, A. M. S. Hamouda, M. H. M. Ahmad, J. Mater. Process. Tech. 178, (2006)29–33.

[8] D. Herlach, P. Galenko, D. Holland-Moritz, Metastable solids from undercooled melts (Elsevier B. V, Germany, 2007).

[9] C. Chaussin, G. Hilly, Métallurgie: alliages métalliques (DUNOD, Paris, 1976).

[10] G. Lesoult, Techniques de l'ingénieurM58, (1986).

[11] M. Colombié, and Coll, Matériaux industriels: matériaux métalliques (DUNOD, Paris, 2000).

[12] C. Rieker, D. G. Morris, Acta. Metal. Mater.38, (1990)1037-1043.

[13] D. A. Porter, K. E. Easterling, Phases transformations in metals and alloys (Taylor & Francis Group, USA, 2004).

[14] W. Kurz, D. J. Fisher, Fundamentals of solidification (Trans Tech Publications Ltd, Vetikon-Zurich, 1998).

[15] S. H. Davis, Theory of solidification (Cambridge University Press, New York, 1949).

[16] M. Wu, J. Li, A. Ludwig, A. Kharicha, Comput. Mater. Sci.92, (2014)267–285.

[17] E. N. De Souza, N. Cheung, A. Garcia, J. Alloys & Compounds, 399, (2005)110–117.

[18] S. Guruswamy, Engineering properties and applications of lead alloys (Marcel Dekker, USA, 2000).

[19] M. Farooq, M.T. Rahim, S. Islam, A.M. Siddiqui, J. Ass. Arab. Univ. Basic & App. Sci.14, (2013)9–18.

[20] S. Heurtault, J. M. Badie, A. Rouanet, G. Arnaud, J. Heat & Mass Transfer, 25, (1982)1671-1676.

[21] D. Li, R. Li, P. Zhang, Sci. in China Ser. A. Mathematics, 47, (2004)41-52.

[22] Z. Radovic, M. Lalovic, J. Mater. Process. Tech.160, (2005)156–159.

[23]M. F. Zhu, D.M. Stefanescu, Acta. Mater. 55, (2007)1741–1755.

[24] C. Le Bot, E. Arquis, Intern. J. Therm. Sci.48, (2009)412–420.

[25] P. R. Goulart, K. S. Cruz, J. E. Spinelli, I. L. Ferreira, N. Cheung, A. Garcia, J. Alloys& Compounds470, (2009)589–599.

[26] H. K. Versteeg, W. Malasekera, An introduction to computational fluid dynamics: The finite volume method (Longman Group Ltd, USA, 1995).
[27] L. Ferreira, V. R. Voller, B. Nestler, A. Garcia, Comput. Mater. Sci.46, (2009)358–366.
[28] F. Mahdi, S. R. Aslan, M. H. Ali, Int J. of thermal Environment engineering, 13 (2016)59-66.
[29] J. N. Silva, D. J. Moutinho, L. Moreira, I. L. Ferreira, O. L. Rocha, J. alloys& Compounds.478, (2009)358-366.
[30] Y. SUN, H. ZHENG, N. Zhang and X. TIAN, ISIJ Internationale, 50, 12 (2010)1875-1878
[31] W. EWA, S. Tomasz, Journal of Applied Mathematics and Computional Mechanics, 13(2) (2014)135-140.
[32] G.M. Stiven, D.R. Sowares, E.P. Oliviera and E.F. lins, Thermal Engineering, Vol 17 (2) (2018)80-86.